



Biomechanical assessment of a passive back exoskeleton using vision-based motion capture and virtual modeling

Yuan Zhou , JoonOh Seo *, Yue Gong, Kelvin HoLam Heung, Masood Khan , Ting Lei 

The Hong Kong Polytechnic University, Hung Hom, Hong Kong Special Administrative Region

ARTICLE INFO

Keywords:

Motion capture
Virtual validation
Biomechanical analysis
Back support exoskeleton
Object lifting

ABSTRACT

This paper proposes a video-driven biomechanical analysis method for measuring muscular loads influenced by wearing an exoskeleton suit, combining vision-based motion capture and virtual modeling approaches. Motion data obtained from site videos is integrated with a newly developed human-exoskeleton model in biomechanical software, to simulate muscular loads on the human body and evaluate exoskeleton suits. This method has been validated through experimental tests, where simulated and directly measured muscle activations were compared for four types of lifting tasks. The results indicate that this method successfully estimates neuromuscular activations of the low back muscles with and without wearing an exoskeleton suit, though the effect of the exoskeleton suit tends to be overestimated in simulations. Despite this limitation, the proposed method is expected to assist in efficiently evaluating exoskeleton use in practice, thereby facilitating the more widespread adoption of passive exoskeletons in construction.

1. Introduction

The construction industry is one of the most labor-intensive sectors, with a large portion of tasks performed manually. As a result, construction workers frequently face physically demanding tasks and awkward postures, leading to musculoskeletal injuries. It is reported that 20% of non-fatal injuries among construction workers are associated with work-related musculoskeletal disorders [1]. Additionally, the nature of manual handling tasks in construction has been identified as a contributing factor to low labor productivity [2]. Although the industry has sought to adopt new technologies such as modular integrated construction, automated systems, or construction robots to reduce the need for manual labor, the use of these technologies remains limited depending on project types, trades, and tasks. Consequently, manual tasks are still prevalent in practice.

Recently, wearable robots such as exoskeleton suits have gained attention in many labor-intensive industries, including construction, to address workers' performance and safety issues. Compared to active systems that require actuators and power supplies, passive exoskeleton suits rely on non-powered mechanical components (e.g., springs or elastic straps), making them lighter, more flexible, and less expensive [3,4]. These features offer comparative advantages for construction workers who need to use them in an unstructured and dynamically changing work environment like construction sites. These wearable robots, designed for specific body parts (e.g., back, shoulders, and knees),

can enhance the physical capabilities of human workers, significantly reducing biomechanical loads. Previous studies investigating their effectiveness have found that they can relieve the risk of musculoskeletal injuries [5] and improve productivity [6]. With the increasing need for passive exoskeletons, many commercially available suits have entered the market, providing more opportunities for practitioners to benefit from these technologies.

Despite the reported benefits, the adoption of passive exoskeleton suits in the construction industry remains limited. One of the challenges hindering their practical application is the lack of comprehensive assessments to prove their applicability at construction sites and to guide the selection of appropriate types of passive exoskeleton suits for specific trades. Most previous studies have focused on laboratory experiments or controlled field settings to evaluate exoskeleton suits using biomechanical or physiological measures such as muscle activations [7], maximum oxygen uptake (VO_2 Max) [8], and heart rates [9]. However, these approaches have been criticized for their invasiveness and the lack of comprehensive measures for assessing the performance of exoskeleton suits [10]. To address these challenges, previous research has incorporated advanced biomechanical simulation tools (e.g., OpenSim, Anybody) [11–13]. These tools enable the estimation of biomechanical metrics such as muscle activity, joint moments, and energy consumption by integrating kinematic data from motion capture systems with virtual models of human-exoskeleton

* Corresponding author.

E-mail address: joonoh.seo@polyu.edu.hk (J. Seo).

systems. Recent empirical studies comparing muscle load reduction due to exoskeleton use have employed both electromyography (EMG) and biomechanical simulations, highlighting the potential of these simulation tools in evaluating the performance of exoskeleton suits [13–15]. Despite the usefulness and validity of simulation-based approaches, the need for sophisticated motion capture systems (e.g., marker-based or inertial measurement unit (IMU)-based systems) to obtain kinematic data may limit the broader application of biomechanical simulation tools, particularly in field settings.

In this regard, this paper aims to propose a non-invasive approach to biomechanically evaluate passive exoskeleton suits at construction sites through a virtual biomechanical simulation driven by in-field motion capture data obtained from video streams. As a proof of concept, this paper focuses on a back exoskeleton suit commonly used by construction workers. Specifically, we propose a computational pipeline for (1) 3-dimensional (3D) modeling of a passive exoskeleton suit combined with a human musculoskeletal system in the biomechanical simulation tool OpenSim [16], (2) virtual simulation of construction tasks using vision-based motion capture data collected at construction sites, and (3) evaluation of muscular loads reduced by wearing an exoskeleton suit. The proposed method is validated by comparing directly measured and simulated muscular loads affected by the use of a passive exoskeleton suit. Based on the results, the potential and remaining challenges of using this method are discussed.

2. Literature review

2.1. Passive exoskeletons and their applications for occupational purposes

Passive exoskeletons provide an effective solution to relieve the physical burden of construction workers performing demanding tasks. The working principles of these exoskeletons vary depending on the type and the body region they support. However, passive exoskeletons generally rely on (1) energy-storing and releasing strategies for gravity compensation and (2) load-transferring mechanisms. For example, most passive exoskeleton systems operate by releasing energy from elastic straps or springs to the wearer in the form of passive torque and force, which partially replaces the wearer's biological muscle activation. Additionally, passive exoskeletons with rigid frames can transfer physical loads from one body part to another through the human-robot interface, thereby reducing muscular loads in more vulnerable body regions.

Passive exoskeletons are typically designed to support specific body parts, and various commercially available suits exist for occupational use, such as (1) Skelex 360-XFR [17], EXHAUSS Stronger [18], Ekso EVO [19], or Hilti EXO-001 [19] for the shoulders, (2) Laveo V2.4, V2.5, Flex [20], Paexo Back [7], BackX [21,22], or FLx ErgoSkeleton [23] for the back, and (3) legX [24] for the knees. Previous studies have evaluated these exoskeletons for different occupational uses. For example, shoulder exoskeletons can support tasks such as overhead assembly [25] and box moving [25]. Back support exoskeletons have been applied to assist with heavy object lifting [26] and manual material handling [20]. Knee exoskeletons are generally used for prolonged squatting activities during tasks such as drilling and welding [24].

In a construction domain, the use of passive exoskeleton suits is relatively new, and recently, several studies have explored the applicability of these suits for construction tasks. Table 1 illustrates the applications and performance evaluation of passive exoskeletons in construction fields. For example, Koopman et al. [26] verified the effect of Laveo 2.4 (back support exoskeleton) in reducing peak compression force, moments, muscle activity during object lifting. Musso et al. [25] tested the performance of a shoulder exoskeleton, Skelex 360-XFR, during the tasks of bricklaying. Results showed that shoulder flexor muscle activation reduces considerably. Baltrusch et al. [27] showed the capability of Skelex 360-XFR in aiding ceiling construction tasks. There are also applications of a knee exoskeleton in cement laying [24].

In addition to these commercial products, recent studies have proposed new designs and mechanical systems for passive exoskeletons to improve performance and minimize user discomfort. For example, Simon et al. [32] proposed a passive back exoskeleton that uses carbon fiber beams instead of springs or elastic bands to accumulate and release elastic energy during back flexion/extension for object lifting. Compared with existing energy storage elements such as gas springs, carbon fiber beams offer advantages like low weight and volume, low energy loss, and potentially high cycle life [33]. Zhang et al. [29] designed a spring-based passive back support exoskeleton to reduce the risk of back injury during manual tasks. Koopman et al. [30] developed a passive back support exoskeleton for object lifting tasks, utilizing a combination of an elastic beam at the back and springs at the hip joints to alleviate the load on the back. Testing results showed a significant reduction in L5/S1 compression forces with device assistance. Additionally, Yin et al. [28] developed a passive shoulder support exoskeleton for manual workers, using two air springs on each side to balance the weight of hand tools.

One recent study proposed an innovative design for biologically inspired back exoskeletons [34]. Inspired by the biological spine, this spine exoskeleton contains three thoracic joints, three lumbar joints, and one caudal joint. Each joint unit includes a ball hinge mechanism and a spring, providing four degrees of freedom. This design helps generate assistive torque during back bending. As these studies suggest, there is considerable room for improving existing passive exoskeleton designs by adopting innovative ideas in terms of design, materials, and mechanical systems. It is expected that new passive exoskeleton systems will continue to become more available in the market.

2.2. Assessment methods for exoskeletons

Occupational exoskeletons, whether passive or active, are designed to support workers in various settings. However, their use must be comprehensively assessed under different conditions to validate their applicability and effectiveness, enabling informed decisions on adoption by practitioners. Previous studies on exoskeleton assessment have focused on: (1) their role in reducing risk factors associated with work-related musculoskeletal disorders, (2) improvements in work performance, (3) reductions in physical effort, and (4) user satisfaction with the exoskeletons [35]. To systematically evaluate exoskeletons, Torricelli et al. [36] proposed a benchmarking framework for wearable robots' performance evaluation, focusing on both functional performance and user experience. While functional performance is evaluated through technological, biomechanical, and physiological indicators, user experience indicators capture perceptual, emotional, and cognitive aspects.

Functional performance assessment of exoskeletons typically relies on direct measurements to gather objective data related to technological, biomechanical, and physiological indicators. Technological indicators evaluate the physical capabilities of exoskeletons, emphasizing their design and mechanical components. One widely used technological indicator is body kinematics, such as range of motion, body angles, or kinematic trajectories, which can be obtained using marker-based full-body motion capture systems in laboratory settings [37]. Analyzing motion capture data provides quantitative assessments of the kinematic compatibility of exoskeleton designs, which significantly affects both functionality and user comfort [36]. Additionally, kinetic measures, such as assistive torque from exoskeletons, directly demonstrate their performance in enhancing the wearer's physical capability [38]. Biomechanical indicators focus on the exoskeleton's impact on the human body through human-exoskeleton interaction. Measuring muscle activations using Electromyography (EMG) is one of the most common methods for understanding the biomechanical performance of exoskeletons. Exoskeletons designed to enhance physical capability can reduce musculoskeletal loads on specific body regions, making the comparison

Table 1
Passive exoskeletons in construction fields.

Study	Device type(s)	Device name(s)	Task(s)	Evaluation methods	Exoskeleton effect(s)
Musso et al. [25]	Shoulder exoskeleton (product ^a)	Skelex 360-XFR	Bricklaying	<ul style="list-style-type: none"> Compare the muscle activity in baseline^b and exoskeleton conditions 	<ul style="list-style-type: none"> Shoulder flexor muscle activation reduced^c considerably
Baltrusch et al. [27]	Shoulder exoskeleton (product)	Skelex 360-XFR	Ceiling construction tasks (drilling, placing, mounting, etc.)	<ul style="list-style-type: none"> Compare the muscle activity in baseline and exoskeleton conditions Survey of user experience 	<ul style="list-style-type: none"> Persistent reductions in shoulder muscle activity of up to 58% Reduced perceived exertion
Yin et al. [28]	Shoulder-support exoskeleton (prototype)	NA ^e	Static and dynamic tool lift experiments	<ul style="list-style-type: none"> Compare the muscle force in baseline and exoskeleton conditions Compare the muscle fatigue in baseline and exoskeleton conditions 	<ul style="list-style-type: none"> A significant decrease in the output force and fatigue in deltoid, biceps brachii, and brachioradialis muscles A significant decrease in the fatigue in above muscles
Koopman et al. [26]	Back support exoskeleton (product)	Laevo 2.4	Static bending and holding tasks	<ul style="list-style-type: none"> Compare the muscle activity in baseline and exoskeleton conditions Compare the L5/S1 moments in baseline and exoskeleton conditions 	<ul style="list-style-type: none"> Significant reductions (11%–57%) in back muscle activity L5/S1 moments significantly reduced
Zhang et al. [29]	Spine exoskeleton (prototype ^d)	NA	Spine flexion and extension tasks	<ul style="list-style-type: none"> Compare the muscle activity in baseline and exoskeleton conditions 	<ul style="list-style-type: none"> Surface Electromyography (sEMG) activation reduced up to 24% at lumbar level sEMG activation reduced up to 54% at thoracic level muscle
Koopman et al. [30]	Back support exoskeleton (prototype)	NA	Object lifting tasks	<ul style="list-style-type: none"> Compare the L5/S1 compression force in baseline and exoskeleton conditions 	<ul style="list-style-type: none"> L5/S1 compression force reduced
Schmalz et al. [7]	Back support exoskeleton (product)	Paexo Back	Object lifting tasks	<ul style="list-style-type: none"> Compare the muscle activity in baseline and exoskeleton conditions Compare the joint force in baseline and exoskeleton conditions Compare metabolic cost in baseline and exoskeleton conditions 	<ul style="list-style-type: none"> Reductions in oxygen rate (9%^f) Reductions in activation of the back and thigh muscles (up to 18%) Reductions in peak and mean compression force at L4/L5 (21%) and L5/S1 (20%)
Gonsalves et al. [21]	Back support exoskeleton (product)	BackX	Formwork fabrication, placing/removing formwork, and concrete finishing	<ul style="list-style-type: none"> Survey of user experience 	<ul style="list-style-type: none"> Reduced stress on the lower back Discomfort at other body parts
Gonsalves et al. [22]	Back support exoskeleton (product)	BackX	Pipework	<ul style="list-style-type: none"> Survey of user experience 	<ul style="list-style-type: none"> Reduced perceived discomfort in the lower back An increase in discomfort at the chest (20%), thigh (73%), and shoulder (250%)
Ogunseju et al. [23]	Back support exoskeleton (product)	FLx ErgoSkeleton	Manual material handling	<ul style="list-style-type: none"> Survey of user experience Compare the kinematics and task completion time in baseline and exoskeleton conditions 	<ul style="list-style-type: none"> Task completion time increased during object lifting The reduced back flexion and increased hip flexion Significant discomfort at the back
Theurel et al. [18]	Upper limb exoskeleton (product)	EXHAUSS Stronger	Load lifting (LIFT), carrying (WALK), and stacking–unstacking (STACK)	<ul style="list-style-type: none"> Compare the muscle activity in baseline and exoskeleton conditions 	<ul style="list-style-type: none"> The deltoid anterior muscle activity significantly reduced during LIFT and STACK The triceps brachii muscle activity significantly decreased during WALK
Bennett et al. [19]	Arm support exoskeletons (products); back support exoskeleton (product)	Ekso EVO and Hilti EXO-001 (arm support); HeroWear Apex (back support)	Pushing/emptying construction gondolas; installing/removing wooden blocks	<ul style="list-style-type: none"> Survey of user experience Compare motions, postures, heart rates, and task completion times in baseline and exoskeleton conditions 	<ul style="list-style-type: none"> The workers responded to the use of exoskeletons differently
Pillai et al. [31]	Knee exoskeleton (Product)	legX	Panel and floor tasks	<ul style="list-style-type: none"> Compare the muscle activity in baseline and exoskeleton conditions 	<ul style="list-style-type: none"> Significant reduction of the rectus femoris activity

Notes:

^a Commercialized product.

^b Without exoskeletons.

^c Compared to baseline condition.

^d Research prototype.

^e Not available.

^f Reduction rate compared to baseline condition.

of muscle activations before and after wearing exoskeletons a straightforward method for validating their performance. While biomechanical

indicators are linked to the effect of exoskeletons on specific body regions, physiological measures, such as energy expenditure or metabolic

demand, indicate the overall impact on the entire body [35]. Energy expenditure is generally measured using an indirect calorimeter that estimates metabolic demands based on respiratory data [39].

User experience assessment is also crucial in determining the suitability of exoskeletons in occupational settings. User experience measurements typically rely on subjective surveys related to perceived benefits, satisfaction, or responses from perceptual, emotional, and cognitive perspectives [36]. Various standardized survey questionnaires have been adopted in previous studies to measure user experience. For example, the Quebec User Evaluation of Satisfaction with Assistive Technology (QUEST) has been used to evaluate user satisfaction with exoskeleton suits [40,41]. It consists of 12 outcome measures that assess satisfaction with a device. Coccia et al. [40] used QUEST to evaluate satisfaction with the arm-support exoskeleton, EXO Paexo Shoulder. The System Usability Scale (SUS), the most widely used standardized questionnaire for assessing perceived usability, is also commonly employed in evaluating user experience with exoskeleton suits. Previous studies have applied SUS to various exoskeleton types, including back support exoskeletons (e.g., FLx ErgoSkeleton, V22 ErgoSkeleton, and Laevo V2.5) [42], and shoulder exoskeletons [43] (e.g., TRL-4). Additionally, Borg's exertion rating scale (Borg CR-20) and NASA-TLX have been used for subjective evaluation of exoskeleton suits such as BackX [44], ShoulderX V2, and Skelex V2 [45].

While these direct or subjective evaluation methods have proven effective in assessing existing exoskeleton suits, simulation-based approaches have also demonstrated their strengths, particularly during the design phase [46]. Biomechanical simulation and analysis using a computerized biomechanical model aims to estimate internal forces (e.g., muscle forces, joint moments) within the human biomechanical system that can rarely be measured directly [47]. A technique known as inverse dynamic analysis based on musculoskeletal models can estimate muscular joint torques required to perform specific tasks with given postures and motions [48]. Following this, muscular forces in various body parts can be computed to achieve required net torques [49]. Although biomechanical parameters (e.g., length, weight, and position of the center of mass of the segments) needed for inverse dynamics can be derived from existing biomechanical models, joint angles must be measured directly. Consequently, previous studies commonly rely on sophisticated motion capture systems to collect kinematic data. This biomechanical simulation approach has been well validated through numerous empirical studies, confirming its efficacy as a non-invasive method for estimating muscle forces [48,50]. With the advent of biomechanical simulation software such as OpenSim [16] and AnyBody [51], an increasing number of researchers are employing simulation-based methodologies by integrating existing biomechanical models with mechanical dynamics of exoskeleton suits to evaluate the extent to which muscular loads can be alleviated through their use. When developing exoskeleton suits, many design factors can influence performance, including mechanical structures, materials, design parameters (e.g., assistive torque), and interfaces between the exoskeleton and the human body. These biomechanical simulation and analysis tools allow for the collection and evaluation of kinematic and kinetic data of human-exoskeleton systems without the need for physical prototypes. Biomechanical features that can be obtained from these tools include joint loading estimation [52], joint moments [53], muscle force [54], metabolic cost [55], ground reaction force [56], and exoskeleton torque [57], enabling more comprehensive biomechanical assessments compared to direct methods used in experimental studies.

Due to these advantages, simulation-based approaches have also been employed to evaluate existing exoskeleton suits. For instance, Zhou et al. [58] used OpenSim to verify the effect of a shoulder exoskeleton in reducing shoulder joint loading during overhead tasks, with similar studies found in [7,15]. Moya-Esteban et al. [52] applied the OpenSim Application Programming Interface (API) to validate the effectiveness of a back support exoskeleton in reducing lumbosacral joint loading and moments during object lifting tasks. Similarly, Schiebl

et al. [59] reported a reduction in shoulder and back torque during exoskeleton-assisted heavy object lifting based on simulation studies using AnyBody. Blanco et al. [14] simulated overhead drilling tasks with upper limb exoskeletons using AnyBody, and their results indicated that the exoskeleton reduced the activation of upper limb muscles. Other simulation studies verifying the effects of exoskeletons in reducing muscle activation are reported in [13,54]. Additionally, there are OpenSim-based simulation studies that verify the effect of exoskeletons in reducing metabolic costs during sitting [55], as well as standing up and walking [60].

However, a critical challenge in using biomechanical simulation and analysis tools in occupational settings is the difficulty of obtaining kinematic data during real-world tasks. Biomechanical loads on the human body continuously change according to dynamic body kinematics and movements, requiring accurate motion data for effective biomechanical simulations. This is why previous studies have relied on sophisticated marker-based motion capture systems in laboratory environments, where occupational tasks are simulated while wearing exoskeleton suits [61,62]. To enable biomechanical simulation and analysis in real-world settings, Seo et al. [63] proposed a motion-data-driven biomechanical analysis for construction tasks using vision-based motion capture approaches. The motion data obtained from site videos was converted into kinematic data in OpenSim, where internal loads, such as muscle force, were estimated to evaluate construction workers' ergonomic risks during tasks at construction sites. The use of vision-based motion capture data would also enable us to evaluate the biomechanical performance of exoskeleton suits without interfering with ongoing construction tasks when combined with human-exoskeleton systems in biomechanical simulation tools (e.g., OpenSim, AnyBody).

3. Methodology

This paper aims to propose a comprehensive framework for biomechanically evaluating the performance of passive exoskeleton suits for construction tasks by combining vision-based motion capture data with virtual modeling of human-exoskeleton systems in the biomechanical simulation tool, OpenSim. While this framework can be applied to any type of exoskeleton device, this paper demonstrates the computational pipeline using one of the most widely used passive back exoskeletons in practice, the Laevo FLEX [20], for which the manufacturer provides detailed specifications and assistive torque data necessary for virtual human-exoskeleton modeling. Fig. 1 provides an overview of the proposed framework, which consists of (1) vision-based motion capture and model reconfiguration for biomechanical simulation, (2) human-exoskeleton system modeling and motion simulation, and (3) muscle-actuated simulation through Computed Muscle Control (CMC) in OpenSim.

3.1. Vision-based motion capture and model reconfiguration for biomechanical simulation

For biomechanical simulation in OpenSim, it is essential to obtain motion data during construction tasks by workers wearing exoskeleton suits, as biomechanical loads on the human body are influenced by body postures and dynamic movements (e.g., body accelerations). As mentioned, previous biomechanical simulation studies have relied on sophisticated marker-based motion capture systems, which are not feasible in field settings. Consequently, motion data has primarily been collected in laboratory environments. To non-invasively capture motion data during ongoing tasks, this paper adopts a vision-based motion capture approach using a monocular camera. Vision-based motion capture and human pose estimation aim to extract body configurations and joint positions from images or videos without the need for markers on the body, often powered by deep learning algorithms such as convolutional neural networks (CNNs). Due to its usefulness

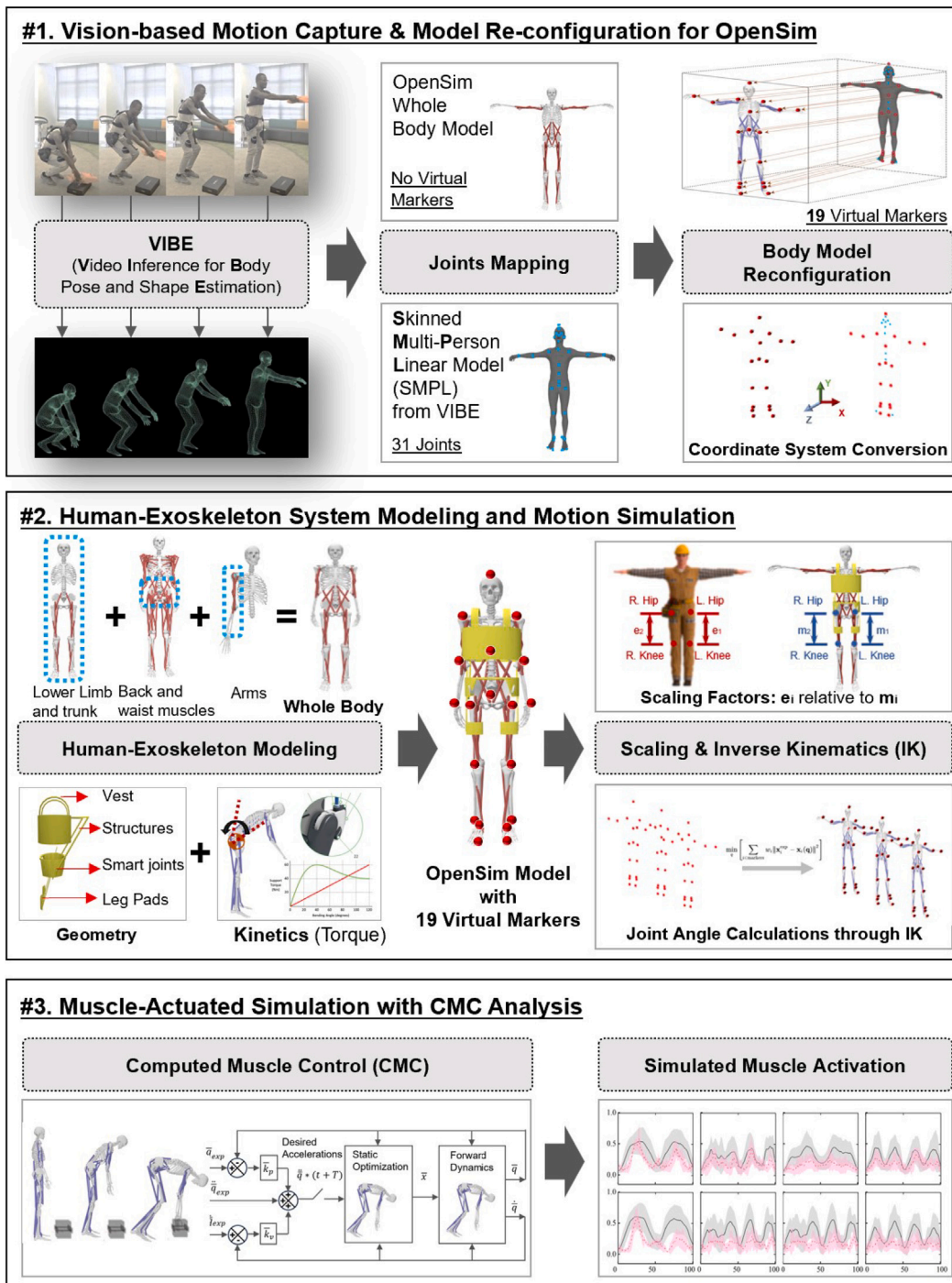


Fig. 1. Research framework.

in understanding human behaviors, vision-based motion capture has been widely used in various fields, including robotics, entertainment, health, and sports sciences [64]. Previous studies have evaluated the accuracy of vision-based motion data compared to traditional marker-based motion capture data, reporting errors in 3D joint positions and joint angles ranging from 45.7 mm to 79.9 mm and from 2.0° to 9.0°, respectively [65]. Although these errors may lead to some inaccuracy in biomechanical simulation and analysis, they are generally insignificant, resulting in less than 10% error in estimating musculoskeletal stresses using biomechanical simulation tools [66]. Considering that EMG-based muscle force estimation typically demonstrates errors ranging from 10% to 20%, it is reasonable to conclude that errors caused by motion data, which are approximately 10%, fall within an acceptable

range [67].

Among the existing vision-based motion capture algorithms, this paper adopts ‘Video Inference for Human Body Pose and Shape Estimation (VIBE)’ developed by Kocabas et al. [68]. VIBE is an advanced algorithm that accurately extracts realistic 3D poses and shapes from single monocular video sequences. One challenge in 3D pose estimation from images is the lack of real training images with ground truth 3D annotations, which can lead to inaccuracies in capturing motion data. To address this issue, VIBE utilizes a large-scale motion capture dataset (AMASS) along with unpaired, in-the-wild videos with 2D key point annotations, achieving better estimation accuracy than other existing algorithms. VIBE has shown joint position errors of approximately

51.9 mm, which is acceptable for biomechanical simulations. An additional advantage of using VIBE is that its output is in the SMPL body model format [69]. The SMPL model represents 3D human motions using various parameters, including a skeleton rig, 3D meshes, and pose blend shapes. Since AMASS, used in VIBE's training, is also in the SMPL format, VIBE can better reflect the variability of human body shapes.

However, OpenSim has been designed to simulate motions by matching experimental markers from marker-based motion capture systems with virtual markers in the OpenSim body model. Therefore, the motion data from VIBE in the SMPL format, which does not include experimental markers, cannot be directly used for simulating motions with the OpenSim body model. To address this, this paper defined 19 new virtual marker positions in the OpenSim body model that correspond to 19 representative joint positions among the 31 body joint positions available from VIBE, as shown at the top of Fig. 1. These 19 representative joints include the pelvis center, right/left shoulder joints, right/left elbow joints, right/left wrist joints, right/left hip joints, right/left knee joints, right/left ankle joints, right/left heels, head top, middle of the spine, and right/left big toes. The joint positions were determined by analyzing the hierarchical structure of joint configurations necessary for motion simulation in OpenSim. However, while some virtual markers in OpenSim are placed on the skin, the joints in VIBE are located at the joint centers. To ensure consistency in marker positions, the virtual markers in OpenSim were adjusted slightly to align with the centers of the joints. Finally, these joint positions from VIBE serve as experimental markers for motion simulation in OpenSim.

Additionally, VIBE extracts joint positional coordinates (x, y, z) that are defined in the camera coordinate system, which differs from the global coordinate system of OpenSim in terms of directions and scales. To align motion data across different coordinate systems, coordinate system and scale transformations have been applied. For example, the transformation from the camera to the global coordinate system in OpenSim can be derived using the following equation:

$$P_g = R \times P_c \quad (1)$$

where P_g and P_c are coordinates of virtual and experimental markers in the global and camera coordinate systems, respectively; R refers to the transformation matrix, which can be described as:

$$R = \begin{bmatrix} 1 & 0 & 0 & t_x \\ 0 & 1 & 0 & t_y \\ 0 & 0 & 1 & t_z \\ 0 & 0 & 0 & 1 \end{bmatrix} \quad (2)$$

where t_x and t_y are coordinates of experimental markers in the camera coordinate system from the VIBE algorithm; t_z is calculated as: [70]

$$t_z = \frac{1}{cam_s} \quad (3)$$

where cam_s is a scale factor extracted from VIBE algorithm.

3.2. Human-Exoskeleton system modeling and motion simulation

The next step involves virtually modeling the human-exoskeleton system, reflecting task characteristics and muscle groups of interest to be evaluated. Generally, OpenSim provides various musculoskeletal models that represent the neuromuscular and musculoskeletal dynamics of the human body for visualizing human movement and analyzing musculoskeletal functions [71]. These models are often designed for specific tasks or body regions, as each model may require different computational assumptions and parameters based on the context of its application.

A back exoskeleton is primarily designed for lifting tasks, which involve muscular activities mainly in the torso, arms, and legs. However, since few existing human body models in OpenSim are well-suited for this study, a modified full-body human model was built by combining and adjusting existing skeleton and muscle models of different body regions, such as arms, trunk, and lower extremities, as shown

Table 2

Human model.		
Component(s)	Sub component(s)	Source model
Arms	Skeleton	Full-body model [72]
	Muscle	Arm26
Head and trunk	Skeleton	Gait10dof18musc
	Muscle	Full-body model [72]
Lower extremity	Skeleton	Gait10dof18musc
	Muscle	Gait10dof18musc

in Table 2. In particular, given that the back exoskeleton is expected to reduce lower back muscular loads, the muscular modeling of other body components was simplified.

Fig. 2 shows the human-exoskeleton model used in this paper. The design of the back exoskeleton and virtual markers were added for graphical representation (Fig. 2(b)) based on the modified full-body model (Fig. 2(a)), while the function of the back exoskeleton (i.e., assistive torque) was computationally modeled (Fig. 2(c)). The back exoskeleton (Laevo FLEX) used in this paper provides dynamic assistive torque from spring systems located at mechanical hip joints. The torque amplitude is related to back bending angles, and the torque-angle curve (maximum torque: 50 N m) is available from the manufacturer [73]. The assistive torque helps lift the torso while transferring the force from the vest to leg pads on the thighs (Fig. 2(c)). This paper assumes that the assistive force acts upward perpendicular to the center of the chest, and the transferred force acts downward perpendicular to the center of the two thighs.

As shown in Fig. 2(c), The amplitudes of the force can be calculated as

$$\begin{cases} F_{chest} = T_{exo}/l_{ch} \\ F_{thigh} = 0.5T_{exo}/l_{ht} \end{cases} \quad (4)$$

where F_{chest} and F_{thigh} are interface force at the chest and thigh, respectively; T_{exo} is the assistive torque from the exoskeleton at a back bending angle of β ($\beta = \alpha_0 - \alpha$); l_{ch} is the distance between the center of the chest and the hip joint; l_{ht} is the distance between the hip joint and the thigh. Additionally, the hand loads during lifting tasks are applied as external loads acting on the human-exoskeleton system, assuming equal loads are exerted on the left and right hands.

The developed human-exoskeleton model with 19 virtual markers is scaled and simulated using motion data from VIBE. As mentioned in the previous step, the relative positions of the virtual markers in the model and joint positions in the VIBE motion data were already matched, but the model should be further scaled to match the subject by adjusting the mass properties and dimensions of the body segments. OpenSim software provides an experimental marker-based scaling tool that adjusts the body model so that the distances between the virtual markers match the distances between the experimental markers. In this paper, the experimental markers are replaced by the joints in the VIBE motion data. After scaling, the inverse kinematics (IK) tool is applied to compute joint angles using VIBE motion data, enabling the exact simulation of the same motions using the human-exoskeleton model.

3.3. Muscle-actuated simulation with CMC analysis

Given the motion and external loads, there are two types of optimization techniques to estimate the muscle activations and forces in OpenSim: static optimization (SO) and Computed Muscle Control (CMC) [74]. The main differences between SO and CMC lie in how they compute the desired accelerations and whether they include passive muscle force contributions. The calculation of desired accelerations is crucial, as OpenSim estimates the muscle activations required to achieve the desired accelerations of body parts. While SO uses the accelerations obtained from experimental data (typically from marker-based motion capture data), CMC adjusts errors using a proportional-derivative control law and also accounts for temporal delays between

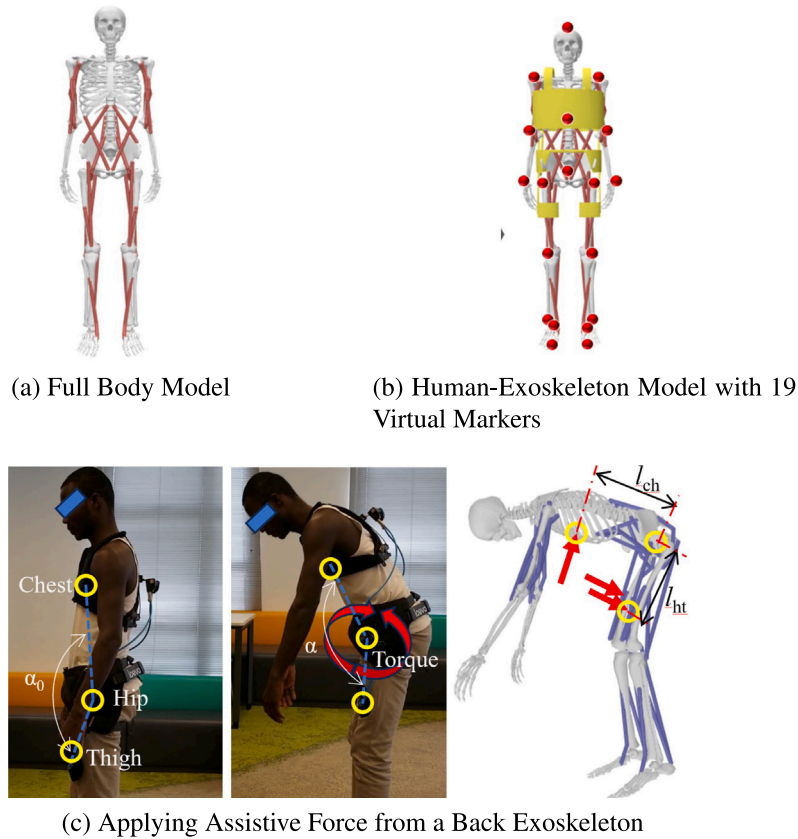


Fig. 2. Human-Exoskeleton system modeling.

muscle activations and force development. The passive muscle force comes from the elastic properties of muscles when they are being stretched [75], which is observed solely in CMC. Although previous studies have extensively examined these methods in the context of walking and running, it remains inconclusive which method is more suitable for lifting tasks. Given that lifting tasks involve rapid body accelerations and that passive muscle forces significantly contribute to spinal loads, this paper utilizes CMC to estimate muscle activations as an indicator of muscular loads, as illustrated in the lower section of Fig. 1.

4. Experimental validation and results

4.1. Experimental protocols

The proposed framework was validated through experimental tests by comparing simulated and measured muscle activations during object lifting tasks with and without wearing a passive back exoskeleton, the Laevo FLEX, used for human exoskeleton modeling. Ten healthy male participants (28.2 ± 2.5 years old, 176.5 ± 7.2 cm, 75 ± 10.6 kg) were recruited for (1) collecting vision-based motion capture data using VIBE to simulate motions and estimate muscle activations (“simulated muscle activation data”) in OpenSim, and (2) measuring actual muscle activations (“experimental muscle activation data”) using wireless sEMG sensors (Biometrics LE230). Before the experiments, all participants gave their informed consent following the procedures approved by the Human Subject Ethics Subcommittee of the Hong Kong Polytechnic University (Reference Number: HSEARS20231101001).

A concrete block weighing 4.1 kg was used for object lifting tasks. Participants were asked to perform four different lifting tasks, including symmetrical stooping (Sym stoop), asymmetrical stooping (Asym stoop), symmetrical squatting (Sym squat), and asymmetrical squatting (Asym squat), both with and without wearing the exoskeleton suit (4

lifting tasks \times 2 conditions = 8 sessions). Fig. 3 shows the four lifting tasks while wearing the exoskeleton suit. The sequence of the 8 sessions was randomized, and a five-minute break was given between sessions for recovery from fatigue.

Two monocular cameras were installed in front of and beside the participants to record videos, which were then processed to obtain motion data using the VIBE algorithm. To enhance accuracy, primary motion data was extracted from the front-facing camera, while motion data from the side view camera supplemented any missing or failed body joint information from the front-facing camera. Four wireless sEMG sensors (Biometrics LE230) were attached to the trunk to measure the activations of four muscle groups: right/left external oblique (REXT/LEXT) and right/left erector spinae (RERC/LERC), as shown in Fig. 4. These muscle groups were selected to evaluate the effectiveness of wearing a passive back exoskeleton in reducing low back loads. Specifically, the erector spinae (ERC) muscles produce the extensor force for object lifting. The external oblique (EXT) muscles are mainly responsible for movement of the trunk and spine. During object lifting, they assist in contracting the abdomen and twisting to the right and left. The ERC muscles, relatively, contribute more power for object lifting tasks [76].

4.2. Data processing

Motion data extracted from videos using the VIBE algorithm were further processed to obtain muscle activations in the four muscle groups (REXT/LEXT and RERC/LERC) using the proposed method in OpenSim. The obtained “simulated muscle activation data” from each participant were normalized by the maximal value among all activation data of each muscle group during the 8 tasks; this is similar to the normalization of EMG data. The results are normalized muscle activations (NMAs). To obtain the muscle activation profiles for each lifting cycle, the data were segmented according to lifting cycles, and the durations

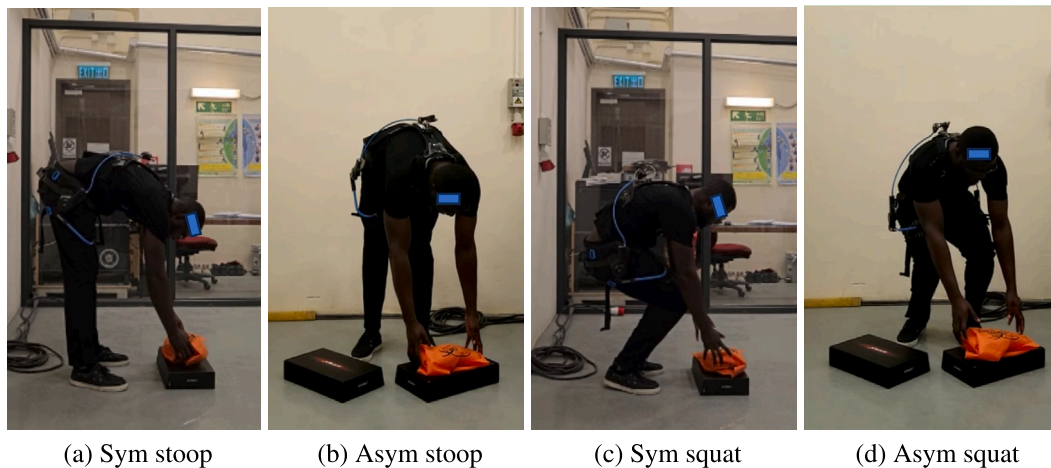


Fig. 3. Four object lifting tasks.

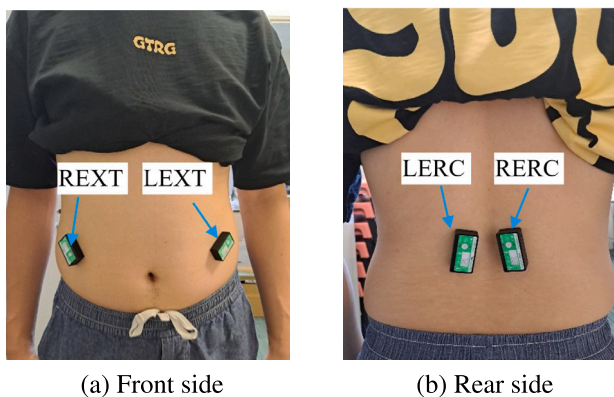


Fig. 4. Installation positions of sEMG sensors.

of each cycle were normalized into a unit of the percentage of a lifting cycle, ranging from 0% to 100%.

Experimental NMAs were obtained by processing raw sEMG signals through the following steps: (1) initial processing, (2) bandpass (BP) filtering, (3) full-wave rectification, (4) root mean square (RMS) envelope, and (5) normalization. These steps follow a typical method for post-processing raw sEMG data [53,77]. Specifically, during initial processing, abnormal signal peaks caused by poor sensor-to-skin connections were removed. Then, the sEMG signals were processed with a BP filter, with high and low cut-off frequencies of 300 Hz and 5 Hz, respectively. Full-wave rectification was applied to make all signal values positive, followed by smoothing the signals using an RMS envelope with a window length of 100 ms. Data segmentation and normalization were also applied in the same way as for the simulated muscle activation data. However, unlike the simulated NMAs, additional curve fitting was applied to the experimental NMAs of ERC muscles to remove abnormal patterns caused by missing data.

4.3. Comparison of simulated and experimental NMAs

Fig. 5 shows the average curves of NMA profiles for four muscle groups under baseline (without wearing an exoskeleton) and exoskeleton (with wearing an exoskeleton) conditions during four lifting tasks. Overall, the simulated NMA profiles (solid black lines) closely match most of the experimental NMA profiles (dotted red lines) in both conditions. However, upon closer examination, it is observed that the simulated and experimental NMA profiles of the EXT muscles show relatively more differences compared to the ERC muscles.

In the baseline condition, the simulated NMA profiles of the left and right ERC muscles exhibit typical load patterns, as reported in previous studies, and match well with the experimental NMA profiles for all four lifting tasks. During Sym stoop (i.e., lifting up and down), it is generally observed that there are two peaks during one lifting cycle, with the peak load from lifting up being higher than the one from lifting down [78]. Both simulated and experimental NMA profiles reflect this pattern. Similarly, during other lifting tasks (i.e., Asym stoop, Sym squat, and Asym squat), the simulated NMA profiles accurately represent the experimental profiles in the baseline condition.

When wearing exoskeletons, both simulated and experimental NMA profiles also show similar results, but there are more deviations in the exoskeleton profiles compared to the baseline profiles. However, the deviations are smaller in the ERC muscles than in the EXT muscles. In general, the external oblique (EXT) muscles tend to behave irregularly, regardless of the type of lifting, weight of the objects, or lifting speed, indicating that the EXT muscles are significantly affected by other factors, including individual muscle control strategies for lifting [79]. Unlike the EXT muscles, muscle activations in the erector spinae (ERC) muscles are more task-specific, making the comparison between simulated and experimental NMAs in ERC muscles more feasible for evaluating the performance of passive exoskeletons.

To quantitatively assess whether the proposed approach accurately simulates actual muscle activations, the mean and peak NMAs for two muscle groups (EXT and ERC, averaged for left and right muscles) during four lifting tasks are summarized in Table 3. In the baseline condition, the mean errors between simulated and experimental NMAs range from -42.4% to $+19.8\%$ for the EXT muscles and from $+7.9\%$ to $+23.8\%$ for the ERC muscles, showing fewer errors in the NMAs of the ERC muscles, as observed in the NMA profiles (Fig. 5). Regarding peak NMAs for the ERC muscles, the simulated NMAs closely predict the experimental NMAs, with errors of $+1.1\%$, -0.6% , and $+2.1\%$ during three lifting tasks (Sym stoop, Sym squat, and Asym squat), although the percentage error ($+22.4\%$) is slightly higher during Asym stoop lifting. These results indicate that the proposed method effectively predicts muscular loads, particularly for the ERC muscles during lifting tasks.

However, when wearing an exoskeleton, the results show larger deviations between simulated and experimental NMAs in both EXT and ERC muscles. The errors for mean NMAs range from $+29.3\%$ to $+89.2\%$ for the EXT muscles and from -27.2% to -10.2% for the ERC muscles. The errors for peak NMAs range from -17.7% to $+44.5\%$ for the EXT muscles and from -54.2% to -47.1% for the ERC muscles. Similar to the baseline condition, larger deviations are observed between simulated and experimental NMAs in the EXT muscles. Although some deviations are also present in the ERC muscles, they are smaller

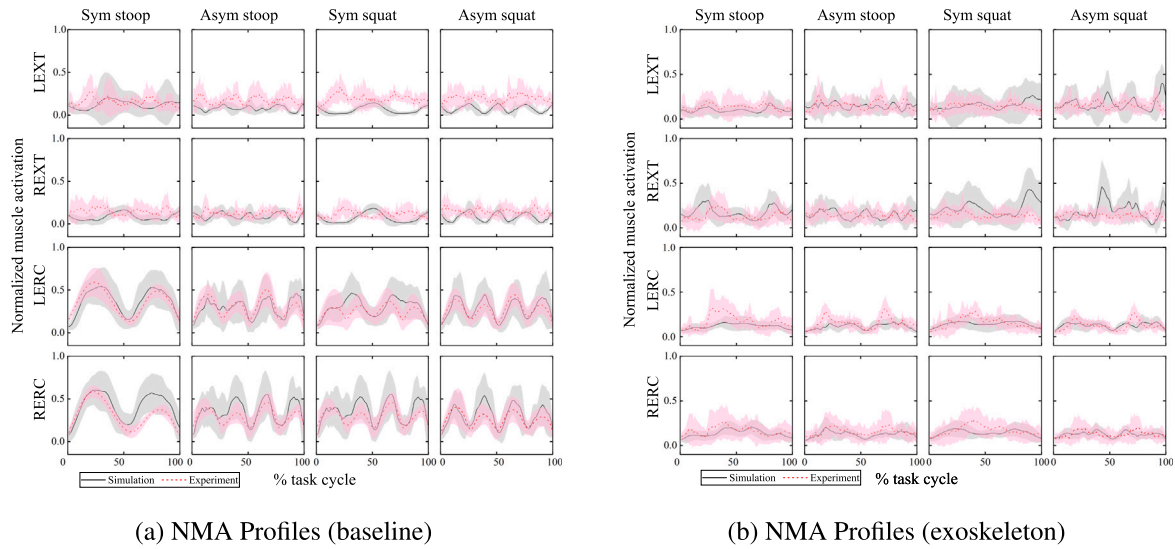


Fig. 5. Experimental and Simulated NMA Profiles.

Table 3
Results of NMAs.

Task condition	Task	Muscles	Mean NMA			Peak NMA		
			Experiment	Simulation	Error	Experiment	Simulation	Error
Baseline	Sym stoop	EXT	0.0997 ± 0.0393	0.1194 ± 0.1173	19.8%	0.4658 ± 0.1972	0.2921 ± 0.2195	-37.3%
		ERC	0.3364 ± 0.0502	0.3949 ± 0.1109	17.4%	0.7648 ± 0.1617	0.7730 ± 0.1867	1.1%
	Asym stoop	EXT	0.1003 ± 0.0297	0.0861 ± 0.0177	-14.2%	0.6323 ± 0.2146	0.616 ± 0.3028	-2.6%
		ERC	0.3011 ± 0.0751	0.3249 ± 0.0754	7.9%	0.6723 ± 0.2065	0.8229 ± 0.1531	22.4%
	Sym squat	EXT	0.1064 ± 0.0415	0.0647 ± 0.0228	-39.2%	0.4762 ± 0.1495	0.1797 ± 0.0544	-62.3%
		ERC	0.2463 ± 0.0621	0.3048 ± 0.1052	23.8%	0.5681 ± 0.1715	0.5648 ± 0.1867	-0.6%
	Asym squat	EXT	0.1124 ± 0.0388	0.0647 ± 0.0228	-42.4%	0.5829 ± 0.2393	0.2337 ± 0.0856	-59.9%
		ERC	0.2712 ± 0.0927	0.2961 ± 0.1051	9.2%	0.6864 ± 0.2153	0.7005 ± 0.2136	2.1%
Exoskeleton	Sym stoop	EXT	0.1033 ± 0.0416	0.1429 ± 0.0601	38.3%	0.4987 ± 0.2101	0.4107 ± 0.1642	-17.7%
		ERC	0.1642 ± 0.0394	0.1290 ± 0.0367	-21.4%	0.4983 ± 0.2328	0.2401 ± 0.0675	-51.8%
	Asym stoop	EXT	0.113 ± 0.0422	0.1461 ± 0.0257	29.3%	0.5676 ± 0.2437	0.583 ± 0.2125	2.7%
		ERC	0.1656 ± 0.0461	0.1205 ± 0.0207	-27.2%	0.6172 ± 0.2509	0.2819 ± 0.0609	-54.3%
	Sym squat	EXT	0.0991 ± 0.0346	0.1875 ± 0.1057	89.2%	0.3978 ± 0.1367	0.5749 ± 0.2538	44.5%
		ERC	0.1590 ± 0.0391	0.1428 ± 0.0449	-10.2%	0.4654 ± 0.1899	0.246 ± 0.0785	-47.1%
	Asym squat	EXT	0.1103 ± 0.0356	0.1748 ± 0.0814	58.9%	0.4788 ± 0.1759	0.6468 ± 0.2297	35.1%
		ERC	0.1541 ± 0.0441	0.1266 ± 0.0246	-17.9%	0.5119 ± 0.1832	0.2531 ± 0.0508	-50.6%

than those in the EXT muscles. More importantly, the simulated NMAs tend to be underestimated compared to the experimental NMAs in the ERC muscles. This may indicate that the effect of wearing a back exoskeleton suit on reducing loads on the ERC muscles is substantially overestimated in OpenSim simulations, resulting in smaller simulated NMA values than experimental NMA values.

To further investigate the effect of wearing an exoskeleton, the mean and peak NMAs in baseline and exoskeleton conditions are summarized in Fig. 6, which also indicates reduction rates from baseline to exoskeleton conditions for all task types. Compared to NMAs in the baseline condition (no exoskeleton), the mean and peak NMAs of the ERC muscles in the exoskeleton condition show significant reductions in both experimental and simulated results, although the extent of these reductions varies depending on the type of lifting tasks. The simulated results show more reductions than the experimental results, with simulated reductions of up to 67.3% for mean NMAs and 68.9% for peak NMAs. However, reductions of 51.2% and 34.8% were observed in the experimental results, which are similar to those from previous studies [80] but smaller than the simulated results. For other lifting tasks (Asym stoop, Sym squat, and Asym squat lifting tasks), reductions in muscle activations were smaller than in stoop lifting tasks, as the direction of assistive torques from the exoskeleton is more suited for stoop

lifting tasks. The amount of reduction in mean and peak NMAs was still more significant in the simulated results than in the experimental results, showing about 16.6% and 44.8% more reductions in mean and peak NMAs, respectively. The potential reasons for overestimating the effect of wearing an exoskeleton in simulations will be discussed further in the following discussion section. In summary, in terms of measuring reductions in NMAs – which would be the most important evaluation metric of exoskeletons – these results suggest that the simulated results may need to be adjusted to reflect real conditions.

5. Discussion

The experimental validation results show that the proposed approach can successfully estimate muscle activations without using invasive sensors such as sEMG electrodes, demonstrating the potential for on-site performance evaluation of passive exoskeletons. The proposed method is particularly effective in predicting the pattern of change in NMA profiles during one cycle of lifting tasks for both baseline and exoskeleton conditions, especially in the ERC muscle groups. The ERC muscles are core paraspinal muscles that mainly contribute to raising the upper body during lifting tasks, and high demands on the ERC muscles are associated with an increased risk of disc prolapse and low

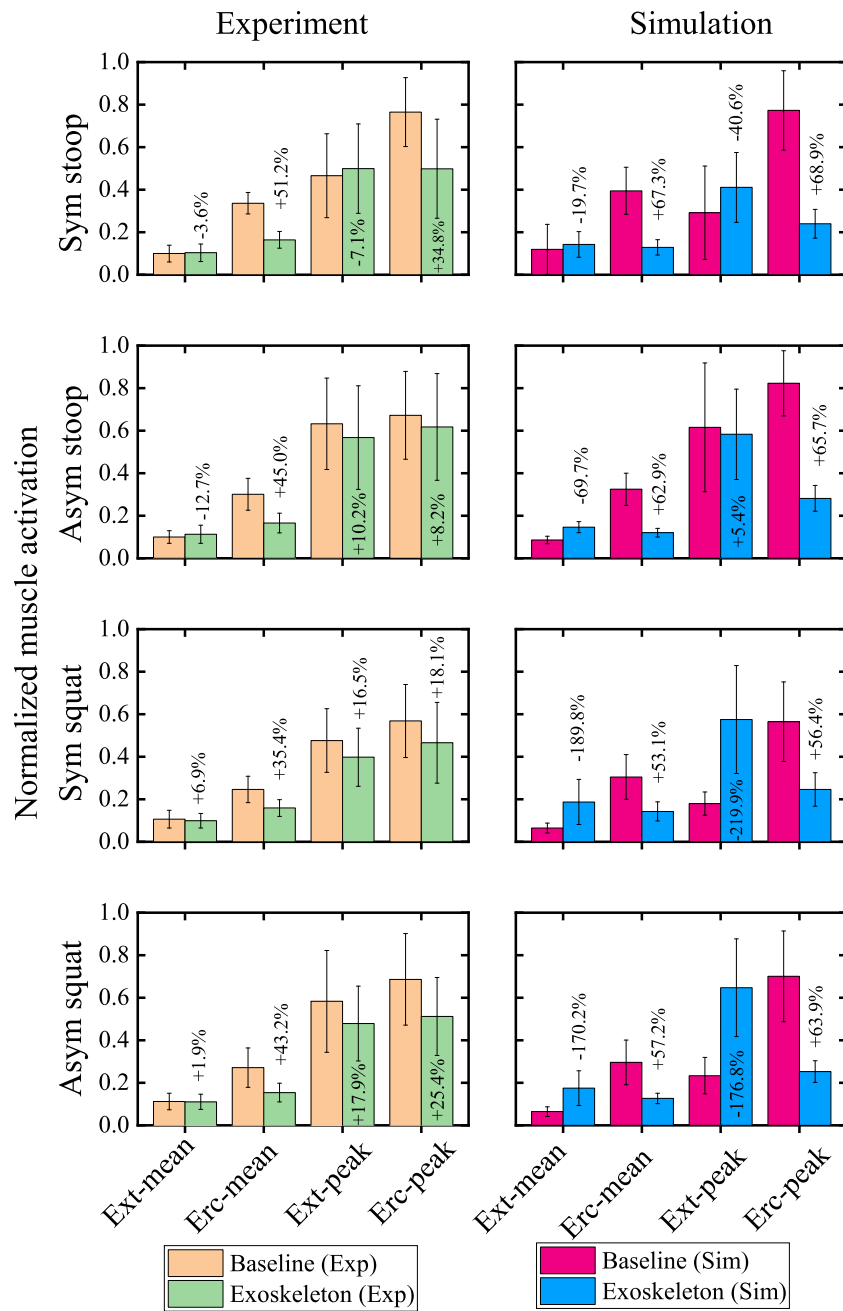


Fig. 6. Mean and peak values of NMA.

back pain [81]. In this regard, predicting NMAs in the ERC muscles is crucial for evaluating the effectiveness of exoskeletons in reducing low back injuries. Errors in predicting mean (+7.9% to +23.8%) and peak (-0.6% to +22.4%) NMAs of the ERC muscles are relatively small in the baseline condition.

However, the errors seem more significant in the exoskeleton condition, with errors ranging from -27.2% to -10.2% for mean NMAs and from -54.2% to -47.1% for peak NMAs. These errors are primarily due to the tendency of OpenSim simulations to overestimate the effect of wearing an exoskeleton in reducing muscular loads, compared with actual conditions, leading to an underestimation of muscle forces exerted on the ERC muscles.

One possible explanation for this result is that OpenSim models assume the force derived from passive springs is used 100% to support lifting tasks, with the remaining force required for lifting tasks being exerted by back muscles. However, in reality, wearers may feel

the assistive force from the exoskeleton but may not fully utilize it, resulting in more muscle force being exerted than necessary. As a result, the reductions in muscle activations from using an exoskeleton are observed to be much less in experimental results than in simulated results.

This suggests that there may be a need for adaptation when using an exoskeleton. As some manufacturers of passive back exoskeletons, such as Laevo FLEX, have stated, it takes time to learn how to use the exoskeletons effectively [20]. Specifically, the limited time available to adapt to a back exoskeleton may affect manual task completion [82] in terms of time and user comfort, and may even increase median/peak activity in thigh, upper back, and knee muscles [83]. Therefore, with sufficient adaptation time to the back support exoskeleton, subjects may use the device more efficiently, and its assistance may better relieve muscle activations during object lifting tasks, as observed in simulation results.

Despite the validity of the proposed method in evaluating muscle activation reductions by exoskeletons, there are still some limitations that require further investigation and refinement. First, self-occlusion (i.e., occlusion of some body joints by other body parts or by an exoskeleton) can frequently occur when collecting motion data, leading to errors in simulating tasks in OpenSim. Although VIBE algorithms can handle self-occlusion issues using extensive training datasets, the impact of wearing an exoskeleton on the accuracy of vision-based motion capture data needs to be further investigated. Second, it is assumed that poor adaptation to an exoskeleton by wearers is the main reason for the underestimated reductions in muscular loads in real conditions. However, this should be further tested through longitudinal studies. Third, the proposed method should be further validated for more dynamic construction tasks involving lifting objects of different sizes and weights.

6. Conclusions

Given the growing prevalence of occupational exoskeletons for aiding manual tasks, the need for evaluating them in practice is indispensable to make sensible adoption decisions. This paper presented a video-driven virtual biomechanical simulation approach to evaluate the assistive performance of a passive back support exoskeleton for construction workers in a non-invasive manner. Without the need for traditional motion capture systems with reflective markers, motion capture data of manual tasks before and after wearing an exoskeleton can be extracted using a vision-based motion capture method (i.e., VIBE algorithms), which can be used to virtually simulate the tasks in a biomechanical simulation tool, OpenSim. In particular, the proposed computational pipeline facilitates the seamless conversion of vision-based motion capture data for biomechanical simulation, taking into account the biomechanical aspects of human-exoskeleton systems.

To simulate muscular activities, a human-exoskeleton model that reflects the kinetic-dynamic interactions between a human body and an exoskeleton has been developed. Given the simulated tasks, the model can estimate muscular loads (i.e., muscle activations). The proposed method has been validated by comparing simulated and experimental muscle activations with and without wearing an exoskeleton. The results indicate that the proposed method can successfully estimate muscle activations of low back muscles during lifting tasks in a baseline condition, showing errors of +7.9% to +23.8% in mean NMAs and -0.6% to +22.4% in peak NMAs of the ERC muscles. However, when wearing an exoskeleton suit, the proposed method consistently estimates muscle forces to be considerably lower than experimental muscle forces across various tasks, thereby overestimating the role of exoskeletons in reducing muscular loads.

Despite some limitations described in the discussion section, the approach could serve as an effective and non-invasive means to not only evaluate existing passive exoskeletons but also provide insights for designing new exoskeletons customized for construction tasks. Existing passive exoskeletons adopt various mechanical and design strategies, but these approaches may not be suitable for construction tasks. When evaluating existing exoskeleton products using the proposed approach, it would be possible to identify potential issues that may arise during exoskeleton use in a construction context, and possible solutions can be quickly assessed by reflecting them in a human-exoskeleton model in OpenSim. As a result, the proposed method can contribute to creating a platform for virtual prototyping to develop new and improved exoskeleton products.

Despite the promising results indicating its effectiveness as a non-invasive method for assessing passive exoskeletons, the proposed approach requires further refinement to address the limitations outlined in the discussion section. For instance, incorporating vision-based motion capture algorithms capable of recovering self-occluded body parts could enhance the accuracy of motion data obtained from video

recordings [84]. Additionally, evaluating human-exoskeleton interactions during practical applications is essential for understanding discrepancies between designed and actual performance, which should be reflected in the virtual modeling of passive exoskeletons.

Addressing these limitations and exploring future directions will position the proposed method as an effective non-invasive tool not only for evaluating existing passive exoskeletons but also for providing insights into the design of customized exoskeletons for construction tasks. While various mechanical and design strategies are currently employed in existing passive exoskeletons, these may not be optimal for construction applications. By utilizing the proposed approach to assess existing exoskeleton products, potential issues arising in a construction context can be identified, allowing for swift evaluation of possible solutions within a human-exoskeleton model in OpenSim. Consequently, this method can contribute to a platform for virtual prototyping aimed at the development of new and enhanced exoskeleton products.

CRedit authorship contribution statement

Yuan Zhou: Writing – original draft, Visualization, Validation, Methodology, Investigation, Formal analysis. **JoonOh Seo:** Writing – review & editing, Validation, Supervision, Resources, Methodology, Conceptualization. **Yue Gong:** Validation, Methodology, Investigation. **Kelvin HoLam Heung:** Writing – review & editing, Resources, Methodology, Conceptualization. **Masood Khan:** Formal analysis, Data curation. **Ting Lei:** Data curation.

Declaration of competing interest

The authors declare the following financial interests/personal relationships which may be considered as potential competing interests: JoonOh SEO reports financial support was provided by The Hong Kong Polytechnic University. If there are other authors, they declare that they have no known competing financial interests or personal relationships that could have appeared to influence the work reported in this paper.

Data availability

Data will be made available on request.

References

- [1] Musculoskeletal disorders in construction, 2024, <https://www.cpwrc.com/research/data-center/data-dashboards/musculoskeletal-disorders-in-construction/>, (Accessed 6 April 2024).
- [2] Z. Zhu, A. Dutta, F. Dai, Exoskeletons for manual material handling—A review and implication for construction applications, *Autom. Constr.* 122 (103493) (2021) 1–11, <http://dx.doi.org/10.1016/j.autcon.2020.103493>.
- [3] A. Voilqué, J. Masood, J. Fauroux, L. Sabourin, O. Guezet, Industrial exoskeleton technology: Classification, structural analysis, and structural complexity indicator, in: 2019 Wearable Robotics Association Conference (WEARRACON), Wearable Robot Assoc, 2019, pp. 13–20, <http://dx.doi.org/10.1109/WEARRACON.2019.8719395>.
- [4] I. Halim, A. Saptari, Z. Abdullah, P. Perumal, M.Z.Z. Abidin, M.N. Muhammad, S. Abdullah, Critical factors influencing user experience on passive exoskeleton application: a review, *Int. J. Integr. Eng.* 14 (4) (2022) 89–115, <http://dx.doi.org/10.30880/ijie.2022.14.04.009>.
- [5] N. Poon, L. van Engelhoven, H. Kazerooni, C. Harris, Evaluation of a trunk supporting exoskeleton for reducing muscle fatigue, *Proc. Hum. Factors Ergon. Soc. Annu. Meet.* 63 (1) (2019) 980–983, <http://dx.doi.org/10.1177/1071181319631491>.
- [6] H.K. Ko, S.W. Lee, D.H. Koo, I. Lee, D.J. Hyun, Waist-assistive exoskeleton powered by a singular actuation mechanism for prevention of back-injury, *Robot. Auton. Syst.* 107 (2018) 1–9, <http://dx.doi.org/10.1016/j.robot.2018.05.008>.
- [7] T. Schmalz, A. Colienne, E. Bywater, L. Fritzsche, C. Gärtner, M. Bellmann, S. Reimer, M. Ernst, A passive back-support exoskeleton for manual materials handling: reduction of low back loading and metabolic effort during repetitive lifting, *IIEE Trans. Occup. Ergon. Hum. Factors* 10 (1) (2022) 7–20, <http://dx.doi.org/10.1080/24725838.2021.2005720>.

- [8] T. Schmalz, J. Schändlinger, M. Schuler, J. Bornmann, B. Schirrmeyer, A. Kannenberg, M. Ernst, Biomechanical and metabolic effectiveness of an industrial exoskeleton for overhead work, *Int. J. Environ. Res. Public Heal.* 16 (23) (2019) 1–12, <http://dx.doi.org/10.3390/ijerph16234792>.
- [9] M. Bär, T. Luger, R. Seibt, M.A. Rieger, B. Steinhilber, Using a passive back exoskeleton during a simulated sorting task: influence on muscle activity, posture, and heart rate, *Hum. Factors* 66 (1) (2024) 40–55, <http://dx.doi.org/10.1177/00187208211073192>.
- [10] L. Fritzsche, P.E. Galibarov, C. Gärtner, J. Bornmann, M. Damsgaard, R. Wall, B. Schirrmeyer, J. Gonzalez-Vargas, D. Pucci, P. Maurice, S. Ivaldi, J. Babic, Assessing the efficiency of exoskeletons in physical strain reduction by biomechanical simulation with AnyBody modeling system, *Wearable Technol.* 2 (2021) 1–16, <http://dx.doi.org/10.1017/wtc.2021.5>.
- [11] B.N. Fournier, E.D. Lemaire, A.J. Smith, M. Doumit, Modeling and simulation of a lower extremity powered exoskeleton, *IEEE Trans. Neural Syst. Rehabil. Eng.* 26 (8) (2018) 1596–1603, <http://dx.doi.org/10.1109/TNSRE.2018.2854605>.
- [12] H. Aftabi, R. Nasiri, M.N. Ahmadabadi, Simulation-based biomechanical assessment of unpowered exoskeletons for running, *Sci. Rep.* 11 (1) (2021) 1–12, <http://dx.doi.org/10.1038/s41598-021-89640-3>.
- [13] Y.-K. Kong, K.-H. Choi, M.-U. Cho, S.-Y. Kim, M.-J. Kim, J.-W. Shim, S.-S. Park, K.-R. Kim, M.-T. Seo, H.-S. Chae, H.-H. Shim, Ergonomic assessment of a lower-limb exoskeleton through electromyography and anybody modeling system, *Int. J. Environ. Res. Public Heal.* 19 (13) (2022) 1–15, <http://dx.doi.org/10.3390/ijerph19138088>.
- [14] A. Blanco, J.M. Catalán, J.A. Díez, J.V. García, E. Lobato, N. García-Aracil, Electromyography assessment of the assistance provided by an upper-limb exoskeleton in maintenance tasks, *Sensors* 19 (15) (2019) 1–20, <http://dx.doi.org/10.3390/s19153391>.
- [15] S. Madinei, M.A. Nussbaum, Estimating lumbar spine loading when using back-support exoskeletons in lifting tasks, *J. Biomech.* 147 (2023) 1–7, <http://dx.doi.org/10.1016/j.jbiomech.2023.111439>.
- [16] OpenSim, 2024, <https://simtk.org/projects/opensim>, (Accessed 30 January 2024).
- [17] Skelex exoskeletons, 2024, <https://www.skelex.com/products>, (Accessed 18 April 2024).
- [18] J. Theurel, K. Desbrosses, T. Roux, A. Savaescu, Physiological consequences of using an upper limb exoskeleton during manual handling tasks, *Appl. Ergon.* 67 (2018) 211–217, <http://dx.doi.org/10.1016/j.apergo.2017.10.008>.
- [19] S.T. Bennett, W. Han, D. Mahmud, P.G. Adamczyk, F. Dai, M. Wehner, D. Veeramani, Z. Zhu, Usability and biomechanical testing of passive exoskeletons for construction workers: A field-based pilot study, *Buildings* 13 (3) (2023) 1–20, <http://dx.doi.org/10.3390/buildings13030822>.
- [20] Laevo exoskeletons, 2023, <https://www.laevo-exoskeletons.com/flex>, (Accessed 12 October 2023).
- [21] N.J. Gonsalves, A. Yusuf, O. Ogunseju, A. Akanmu, Evaluation of concrete workers' interaction with a passive back-support exoskeleton, *Eng. Constr. Archit. Manag.* 31 (11) (2024) 4585–4601, <http://dx.doi.org/10.1108/ECAM-12-2022-1156>.
- [22] N. Gonsalves, A. Akanmu, X. Gao, P. Agee, A. Shojaei, Industry perception of the suitability of wearable robot for construction work, *J. Constr. Eng. Manag.* 149 (5) (2023) 1–12, <http://dx.doi.org/10.1061/JCEM4.COENG-12762>.
- [23] O. Ogunseju, J. Olayiwola, A. Akanmu, O.A. Olatunji, Evaluation of postural-assist exoskeleton for manual material handling, *Eng. Constr. Archit. Manag.* 29 (3) (2022) 1358–1375, <http://dx.doi.org/10.1108/ECAM-07-2020-0491>.
- [24] V3 LEGX, 2024, <https://www.westonrobot.com/leg-protection-exoskeleton-legx>, (Accessed 10 May 2024).
- [25] M. Musso, A.S. Oliveira, S. Bai, Influence of an upper limb exoskeleton on muscle activity during various construction and manufacturing tasks, *Appl. Ergon.* 114 (2024) 1–8, <http://dx.doi.org/10.1016/j.apergo.2023.104158>.
- [26] A.S. Koopman, I. Kingma, M.P. de Looze, J.H. van Dieën, Effects of a passive back exoskeleton on the mechanical loading of the low-back during symmetric lifting, *J. Biomech.* 102 (2020) 1–8, <http://dx.doi.org/10.1016/j.jbiomech.2019.109486>.
- [27] S.J. Baltrusch, F. Krause, A.W. de Vries, M.P. de Looze, Arm-support exoskeleton reduces shoulder muscle activity in ceiling construction, *Ergonomics* 67 (8) (2023) 1051–1063, <http://dx.doi.org/10.1080/00140139.2023.2280443>.
- [28] P. Yin, L. Yang, S.G. Qu, Development of an ergonomic wearable robotic device for assisting manual workers, *Int. J. Adv. Robot. Syst.* 18 (5) (2021) 1–11, <http://dx.doi.org/10.1177/17298814211046745>.
- [29] H. Zhang, A. Kadrolkar, F.C. Sup IV, Design and preliminary evaluation of a passive spine exoskeleton, *J. Med. Dev.* 10 (1) (2016) 1–8, <http://dx.doi.org/10.1115/1.4031798>.
- [30] A.S. Koopman, M. Näf, S.J. Baltrusch, I. Kingma, C. Rodriguez-Guerrero, J. Babic, M.P. de Looze, J.H. van Dieën, Biomechanical evaluation of a new passive back support exoskeleton, *J. Biomech.* 105 (2020) 1–8, <http://dx.doi.org/10.1016/j.jbiomech.2020.109795>.
- [31] M.V. Pillai, L. Van Engelshoven, H. Kazerooni, Evaluation of a lower leg support exoskeleton on floor and below hip height panel work, *Hum. Factors* 62 (3) (2020) 489–500, <http://dx.doi.org/10.1177/0018720820907752>.
- [32] A.A. Simon, M.M. Alemi, A.T. Asbeck, Kinematic effects of a passive lift assistive exoskeleton, *J. Biomech.* 120 (2021) 1–11, <http://dx.doi.org/10.1016/j.jbiomech.2021.110317>.
- [33] S.E. Chang, T. Pesek, T.R. Pote, J. Hull, J. Geissinger, A.A. Simon, M.M. Alemi, A.T. Asbeck, Design and preliminary evaluation of a flexible exoskeleton to assist with lifting, *Wearable Technol.* 1 (2020) 1–22, <http://dx.doi.org/10.1017/wtc.2020.10>.
- [34] J. Song, A. Zhu, Y. Tu, J. Zou, Multijoint passive elastic spine exoskeleton for stoop lifting assistance, *Int. J. Adv. Robot. Syst.* 18 (6) (2021) 1–13, <http://dx.doi.org/10.1177/17298814211062033>.
- [35] S. De Bock, J. Ghillebert, R. Govaerts, B. Tassignon, C. Rodriguez-Guerrero, S. Crea, J. Veneman, J. Geeroms, R. Meeusen, K. De Pauw, Benchmarking occupational exoskeletons: An evidence mapping systematic review, *Appl. Ergon.* 98 (2022) 1–19, <http://dx.doi.org/10.1016/j.apergo.2021.103582>.
- [36] D. Torricelli, C. Rodriguez-Guerrero, J.F. Veneman, S. Crea, K. Briem, B. Lenggenhager, P. Beckerle, Benchmarking wearable robots: challenges and recommendations from functional, user experience, and methodological perspectives, *Front. Robot. AI* 7 (2020) 1–7, <http://dx.doi.org/10.3389/frobt.2020.561774>.
- [37] M.B. Näf, K. Junius, M. Rossini, C. Rodriguez-Guerrero, B. Vanderborght, D. Lefeber, Misalignment compensation for full human-exoskeleton kinematic compatibility: State of the art and evaluation, *Appl. Mech. Rev.* 70 (5) (2018) 1–19, <http://dx.doi.org/10.1115/1.4042523>.
- [38] S. Madinei, S. Kim, J.-H. Park, D. Srinivasan, M.A. Nussbaum, A novel approach to quantify the assistive torque profiles generated by passive back-support exoskeletons, *J. Biomech.* 145 (2022) 1–7, <http://dx.doi.org/10.1016/j.jbiomech.2022.111363>.
- [39] M.M. Alemi, S. Madinei, S. Kim, D. Srinivasan, M.A. Nussbaum, Effects of two passive back-support exoskeletons on muscle activity, energy expenditure, and subjective assessments during repetitive lifting, *Hum. Factors* 62 (3) (2020) 458–474, <http://dx.doi.org/10.1177/0018720819897669>.
- [40] A. Coccia, E.M. Capodaglio, F. Amitrano, V. Gabba, M. Panigazzi, G. Pagano, G. D'Addio, Biomechanical effects of using a passive exoskeleton for the upper limb in industrial manufacturing activities: A pilot study, *Sensors* 24 (5) (2024) 1–19, <http://dx.doi.org/10.3390/s24051445>.
- [41] R. van Sluijs, T. Scholtysik, A. Brunner, L. Kuoni, D. Bee, M. Kos, V. Bartenbach, O. Lamberg, Design and evaluation of the OmniSuit: A passive occupational exoskeleton for back and shoulder support, *Appl. Ergon.* 120 (2024) 1–9, <http://dx.doi.org/10.1016/j.apergo.2024.104332>.
- [42] J. Hwang, V.N.K. Yerriboina, H. Ari, J.H. Kim, Effects of passive back-support exoskeletons on physical demands and usability during patient transfer tasks, *Appl. Ergon.* 93 (2021) 1–9, <http://dx.doi.org/10.1016/j.apergo.2021.103373>.
- [43] A. van der Have, M. Rossini, C. Rodriguez-Guerrero, S. Van Rossum, I. Jonkers, The Exo4Work shoulder exoskeleton effectively reduces muscle and joint loading during simulated occupational tasks above shoulder height, *Appl. Ergon.* 103 (2022) 1–10, <http://dx.doi.org/10.1016/j.apergo.2022.103800>.
- [44] A. Okunola, A.A. Akanmu, A.O. Yusuf, Comparison of active and passive back-support exoskeletons for construction work: range of motion, discomfort, usability, exertion and cognitive load assessments, *Smart Sustain. Built Environ.* (2023) 1–17, <http://dx.doi.org/10.1108/SASBE-06-2023-0147>.
- [45] S. De Bock, J. Ghillebert, R. Govaerts, S.A. Elprama, U. Marusic, B. Serrien, A. Jacobs, J. Geeroms, R. Meeusen, K. De Pauw, Passive shoulder exoskeletons: More effective in the lab than in the field? *IEEE Trans. Neural Syst. Rehabil. Eng.* 29 (2020) 173–183, <http://dx.doi.org/10.1109/TNSRE.2020.3041906>.
- [46] M. Khamar, M. Edrisi, M. Zahir, Human-exoskeleton control simulation, kinetic and kinematic modeling and parameters extraction, *MethodsX* 6 (2019) 1838–1846, <http://dx.doi.org/10.1016/j.mex.2019.08.014>.
- [47] D.B. Chaffin, A computerized biomechanical model—development of and use in studying gross body actions, *J. Biomech.* 2 (4) (1969) 429–441, [http://dx.doi.org/10.1016/0021-9290\(69\)90018-9](http://dx.doi.org/10.1016/0021-9290(69)90018-9).
- [48] A. Erdemir, S. McLean, W. Herzog, A.J. van den Bogert, Model-based estimation of muscle forces exerted during movements, *Clin. Biomech.* 22 (2) (2007) 131–154, <http://dx.doi.org/10.1016/j.clinbiomech.2006.09.005>.
- [49] Y. Koike, M. Kawato, Estimation of dynamic joint torques and trajectory formation from surface electromyography signals using a neural network model, *Biol. Cybernet.* 73 (4) (1995) 291–300, <http://dx.doi.org/10.1007/s004220050185>.
- [50] D.B. Chaffin, A. Freivalds, S.M. Evans, On the validity of an isometric biomechanical model of worker strengths, *IIE Trans.* 19 (3) (1987) 280–288, <http://dx.doi.org/10.1080/07408178708975397>.
- [51] Anybody technology, 2024, <https://www.anybodytech.com/>, (Accessed 13 August 2024).
- [52] A. Moya-Esteban, G. Durandau, H. van der Kooij, M. Sartori, Real-time lumbosacral joint loading estimation in exoskeleton-assisted lifting conditions via electromyography-driven musculoskeletal models, *J. Biomech.* 157 (2023) 1–9, <http://dx.doi.org/10.1016/j.jbiomech.2023.111727>.
- [53] A. Moya-Esteban, H. van der Kooij, M. Sartori, Robust estimation of lumbar joint forces in symmetric and asymmetric lifting tasks via large-scale electromyography-driven musculoskeletal models, *J. Biomech.* 144 (2022) 1–9, <http://dx.doi.org/10.1016/j.jbiomech.2022.111307>.
- [54] A. Sohane, R. Agarwal, Evaluation of 3D design lower limb exoskeleton on human musculoskeletal with various loads, *Expert Syst.* 38 (7) (2021) 1–12, <http://dx.doi.org/10.1111/esyx.12738>.

- [55] Y.F. Wang, G.R. Zhao, Y.A. Diao, Y. Feng, G.L. Li, Performance analysis of unpowered lower limb exoskeleton during sit down and stand up, *Robotica* 40 (5) (2022) 1274–1292, <http://dx.doi.org/10.1017/S0263574721001077>.
- [56] L. Cao, J.X. Zhang, P. Zhang, D.L. Fang, Research on the influence of exoskeletons on human characteristics by modeling and simulation using the AnyBody modeling system, *Appl. Sci.- Basel* 13 (14) (2023) 1–16, <http://dx.doi.org/10.3390/app13148184>.
- [57] J.M. Li, D.D. Molinaro, A.S. King, A. Mazumdar, A.J. Young, Design and validation of a cable-driven asymmetric back exosuit, *IEEE Trans. Robot.* 38 (3) (2022) 1489–1502, <http://dx.doi.org/10.1109/TRO.2021.3112280>.
- [58] X. Zhou, L. Zheng, Model-based comparison of passive and active assistance designs in an occupational upper limb exoskeleton for overhead lifting, *IIEE Trans. Occup. Ergon. Hum. Factors* 9 (3–4) (2021) 167–185, <http://dx.doi.org/10.1080/24725838.2021.1954565>.
- [59] J. Schiebl, M. Tröster, W. Idoudi, E. Gneiting, L. Spies, C. Maufroy, U. Schneider, T. Bauernhansl, Model-based biomechanical exoskeleton concept optimization for a representative lifting task in logistics, *Int. J. Environ. Res. Public Heal.* 19 (23) (2022) 1–22, <http://dx.doi.org/10.3390/ijerph192315533>.
- [60] S.H. Hu, W.J. Chen, X.Y. Xiong, X.T. Sun, C.D. He, Design and analysis of a passive exoskeleton with its hip joint energy-storage, *Proc. Inst. Mech. Eng. Part H- J. Eng. Med.* 237 (9) (2023) 1039–1051, <http://dx.doi.org/10.1177/09544119231188678>.
- [61] U.L. Erezuma, M.Z. Amilibia, A.E. Elorza, C. Cortés, J. Irazusta, A. Rodriguez-Larrad, A statistical parametric mapping analysis approach for the evaluation of a passive back support exoskeleton on mechanical loading during a simulated patient transfer task, *J. Appl. Biomech.* 39 (1) (2023) 22–33, <http://dx.doi.org/10.1123/jab.2022-0126>.
- [62] S. Auer, M. Tröster, J. Schiebl, K. Iversen, D.S. Chander, M. Damsgaard, S. Dendorfer, Biomechanical assessment of the design and efficiency of occupational exoskeletons with the AnyBody modeling system, *Z. Arbeitswissenschaft* 76 (4) (2022) 440–449, <http://dx.doi.org/10.1007/s41449-022-00336-4>.
- [63] J. Seo, R. Starbuck, S. Han, S. Lee, T.J. Armstrong, Motion data-driven biomechanical analysis during construction tasks on sites, *J. Comput. Civ. Eng.* 29 (4) (2015) 1–13, [http://dx.doi.org/10.1061/\(ASCE\)CP.1943-5487.0000400](http://dx.doi.org/10.1061/(ASCE)CP.1943-5487.0000400).
- [64] Y. Desmarais, D. Mottet, P. Slangen, P. Montesinos, A review of 3D human pose estimation algorithms for markerless motion capture, *Comput. Vis. Image Underst.* 212 (2021) 1–19, <http://dx.doi.org/10.1016/j.cviu.2021.103275>.
- [65] S.L. Colyer, M. Evans, D.P. Cosker, A.I. Salo, A review of the evolution of vision-based motion analysis and the integration of advanced computer vision methods towards developing a markerless system, *Sport. Med.- Open* 4 (2018) 1–15, <http://dx.doi.org/10.1186/s40798-018-0139-y>.
- [66] J. Seo, A. Alwasel, S. Lee, E.M. Abdel-Rahman, C. Haas, A comparative study of in-field motion capture approaches for body kinematics measurement in construction, *Robotica* 37 (5) (2019) 928–946, <http://dx.doi.org/10.1017/S0263574717000571>.
- [67] C.A. Doorenbosch, J. Harlaar, Accuracy of a practicable EMG to force model for knee muscles, *Neurosci. Lett.* 368 (1) (2004) 78–81, <http://dx.doi.org/10.1016/j.neulet.2004.06.055>.
- [68] M. Kocabas, N. Athanasiou, M.J. Black, Vibe: Video inference for human body pose and shape estimation, in: *Proceedings of the IEEE/CVF Conference on Computer Vision and Pattern Recognition*, ISBN: 978-1-7281-7168-5, 2020, pp. 5253–5263, <http://dx.doi.org/10.1109/CVPR42600.2020.00530>.
- [69] M. Loper, N. Mahmood, J. Romero, G. Pons-Moll, M.J. Black, SMPL: A skinned multi-person linear model, *ACM Trans. Graph.* 34 (6) (2015) 851–866, <http://dx.doi.org/10.1145/2816795.2818013>.
- [70] Direct 3d human pose and shape estimation, 2021, <https://github.com/ikvision/ikvision.github.io/blob/master/README.md#5-predicted-camera-parameters>, (Accessed 10 February 2024).
- [71] A. Falisse, S. Van Rossom, J. Gijssbers, F. Steenbrink, B.J. van Basten, I. Jonkers, A.J. van den Bogert, F. De Groot, OpenSim versus human body model: a comparison study for the lower limbs during gait, *J. Appl. Biomech.* 34 (6) (2018) 496–502, <http://dx.doi.org/10.1123/jab.2017-0156>.
- [72] G. Marije, J. Ilse, B. Sjoerd, v.D. Jaap, Analysis of arm swing during human walking, 2014, https://simtk.org/projects/arm_swing/, (Accessed 1 August 2023).
- [73] V. Van Harmelen, J. Schnieders, S. Wagemaker, *Measuring the amount of support of lower back exoskeletons*, Laevo White Paper, 2022.
- [74] S.A. Roelker, E.J. Caruthers, R.K. Hall, N.C. Pelz, A.M. Chaudhari, R.A. Siston, Effects of optimization technique on simulated muscle activations and forces, *J. Appl. Biomech.* 36 (4) (2020) 259–278, <http://dx.doi.org/10.1123/jab.2018-0332>.
- [75] T.K. Koo, J.-Y. Guo, J.H. Cohen, K.J. Parker, Relationship between shear elastic modulus and passive muscle force: an ex-vivo study, *J. Biomech.* 46 (12) (2013) 2053–2059, <http://dx.doi.org/10.1016/j.jbiomech.2013.05.016>.
- [76] A. Cresswell, A. Thorstensson, Changes in intra-abdominal pressure, trunk muscle activation and force during isokinetic lifting and lowering, *Eur. J. Appl. Physiol.* 68 (4) (1994) 315–321, <http://dx.doi.org/10.1007/BF00571450>.
- [77] D. Levine, J. Richards, M. Whittle, *Whittle's Gait Analysis, Fifth Edition*, 978-0-7020-4265-2, Elsevier, ISBN, 2012.
- [78] D.A. Quirk, J. Chung, G. Schiller, J.M. Cherin, P. Arens, D.A. Sherman, E.R. Zeligson, D.M. Dalton, L.N. Awad, C.J. Walsh, Reducing back exertion and improving confidence of individuals with low back pain with a back exosuit: A feasibility study for use in BACPAC, *Pain Med.* 24 (SI) (2023) S175–S186, <http://dx.doi.org/10.1093/pm/pnad003>.
- [79] I. Vahdat, M. Rostami, F.T. Ghomshesh, S. Khorramyeh, A. Tanbakooz, The effects of task execution variables on the musculature activation strategy of the lower trunk during squat lifting, *Int. J. Ind. Ergon.* 55 (2016) 77–85, <http://dx.doi.org/10.1016/j.ergon.2016.07.007>.
- [80] M.I.M. Refai, A. Moya-Esteban, L. van Zijl, H. van der Kooij, M. Sartori, Benchmarking commercially available soft and rigid passive back exoskeletons for an industrial workplace, *Wearable Technol.* 5 (2024) 1–16, <http://dx.doi.org/10.1017/wtc.2024.2>.
- [81] P. Dolan, M. Adams, The relationship between EMG activity and extensor moment generation in the erector spinae muscles during bending and lifting activities, *J. Biomech.* 26 (4–5) (1993) 513–522, [http://dx.doi.org/10.1016/0021-9290\(93\)90013-5](http://dx.doi.org/10.1016/0021-9290(93)90013-5).
- [82] T. Luger, M. Bär, R. Seibt, M.A. Rieger, B. Steinhilber, Using a back exoskeleton during industrial and functional tasks—Effects on muscle activity, posture, performance, usability, and wearer discomfort in a laboratory trial, *Hum. Factors* 65 (1) (2023) 5–21, <http://dx.doi.org/10.1177/00187208211007267>.
- [83] T. Luger, M. Baer, R. Seibt, P. Rimmele, M.A. Rieger, B. Steinhilber, A passive back exoskeleton supporting symmetric and asymmetric lifting in stoop and squat posture reduces trunk and hip extensor muscle activity and adjusts body posture—A laboratory study, *Appl. Ergon.* 97 (2021) 1–10, <http://dx.doi.org/10.1016/j.apergo.2021.103530>.
- [84] L. Malekian, R. Lapeer, *Self-Occluded Human Pose Recovery in Monocular Video Motion Capture*, 2024, pp. 1–6, <http://dx.doi.org/10.1109/ICPR562101.2024.10677815>, 14th International Conference on Pattern Recognition Systems (ICPRS), London, ENGLAND, JUL 15-18, 2024.